ORIGINAL ARTICLE

JBMR®

Indirubin-3′-Oxime Reverses Bone Loss in Ovariectomized and Hindlimb-Unloaded Mice Via Activation of the Wnt/β-Catenin Signaling

Muhammad Zahoor,[1,2] Pu-Hyeon Cha,[1,2] Do Sik Min,[1,3] and Kang-Yell Choi[1,2]

[1]Translational Research Center for Protein Function Control, College of Life Science and Biotechnology, Yonsei University, Seoul, South Korea
[2]Department of Biotechnology, College of Life Science and Biotechnology, Yonsei University, Seoul, South Korea
[3]Department of Molecular Biology, College of Natural Science, Pusan National University, Pusan, South Korea

ABSTRACT

Osteoporosis is a major global health issue in elderly people. Because Wnt/β-catenin signaling plays a key role in bone homeostasis, we screened activators of this pathway through cell-based screening, and investigated indirubin-3′-oxime (I3O), one of the positive compounds known to inhibit GSK3β, as a potential anti-osteoporotic agent. Here, we show that I3O activated Wnt/β-catenin signaling via inhibition of the interaction of GSK3β with β-catenin, and induced osteoblast differentiation in vitro and increased calvarial bone thickness ex vivo. Intraperitoneal injection of I3O increased bone mass and improved microarchitecture in normal mice and reversed bone loss in an ovariectomized mouse model of age-related osteoporosis. I3O also increased thickness and area of cortical bone, indicating improved bone strength. Enhanced bone mass and strength correlated with activated Wnt/β-catenin signaling, as shown by histological analyses of both trabecular and cortical bones. I3O also restored mass and density of bone in hindlimb-unloaded mice compared with control, suspended mice, demonstrating bone-restoration effects of I3O in non-aged–related osteoporosis as well. Overall, I3O, a pharmacologically active small molecule, could be a potential therapeutic agent for the treatment and prevention of osteoporosis. © 2014 American Society for Bone and Mineral Research.

KEY WORDS: GSK3β INHIBITOR; INDIRUBIN-3′-OXIME; OSTEOPOROSIS; OVARIECTOMY; WNT/β-CATENIN SIGNALING PATHWAY

Introduction

Osteoporosis is the most common bone disease and is considered a major public health problem worldwide.[1] Low bone mass and weakened microarchitecture in osteoporosis increase vulnerability to fractures and cause debilitating bone pain in the elderly.[2] Fracture in osteoporotic individuals is accompanied by high rates of morbidity and mortality[3,4] that are estimated to double by 2050.[5] Estrogen depletion during menopause is a major cause of age-related osteoporosis, resulting from accelerated bone resorption and a systemic calcium (Ca) imbalance,[6] whereas extended exposure to microgravity[7] and prolonged bed rest also cause bone deterioration, resulting in non-age–related osteoporosis.[8]

The Wnt/β-catenin pathway is known to be involved in bone homeostasis by regulating osteoblastogenesis and osteoclastogenesis.[9] Activation of Wnt/β-catenin signaling is initiated by the binding of a Wnt ligand to a dual-receptor complex composed of low-density lipoprotein receptor-related protein 5 or 6 (LRP5/6) and the seven-transmembrane domain receptor, Frizzled. Evidence for direct roles of Wnt/β-catenin signaling in bone formation is shown by decreased bone mass and density in a mouse model with LRP5 loss-of-function mutation[10] and increased osteoblast differentiation and high bone mass in a mouse with LRP5 gain-of-function mutation.[11]

The significance of Wnt/β-catenin signaling is also evident in bone resorption; expression of a constitutively active β-catenin mutant under control of the *COL1A1* promoter results in defective osteoclastogenesis,[12] and β-catenin deletion in mature osteoblasts results in high tartrate-resistant acid phosphatase (TRAP) activity.[12,13] Although the role of aberrantly activated Wnt/β-catenin signaling is associated with development of various cancers,[14] involvement of Wnt/β-catenin signaling in osteosarcoma has not been established so far.[15] Therefore, the Wnt/β-catenin pathway appears to be an attractive target for the development of anti-osteoporosis drugs. Although antibodies that neutralize Wnt/β-catenin pathway-activating molecules, including secreted frizzled-related protein-1 (sFRP1), sclerostin, and dickkopf-1 (DKK1), have been tested as possible therapeutics for the treatment of osteoporosis,[16,17] no anti-osteoporotic drug targeting Wnt/β-catenin signaling is clinically available.

Here, we identified and characterized a pharmacologically active chemical, indirubin-3′-oxime (I3O), as an agent that

Received in original form October 3, 2013; revised form November 5, 2013; accepted November 12, 2013. Accepted manuscript online November 16, 2013.
Address correspondence to: Kang-Yell Choi, PhD, Department of Biotechnology, College of Life Science and Biotechnology, Yonsei University, 50 Yonsei Ro, Seodemun-Gu, Seoul, South Korea 120-749. E-mail: kychoi@yonsei.ac.kr
Additional Supporting Information may be found in the online version of this article.

Journal of Bone and Mineral Research, Vol. 29, No. 5, May 2014, pp 1196–1205
DOI: 10.1002/jbmr.2147

induces osteoblast differentiation and inhibits osteoclast differentiation in vitro. We also characterized I3O as an agent that reverses bone loss resulting from ovariectomy, indicating its potential for development as an anti-osteoporosis drug.

Materials and Methods

Cell culture and reagents

Human embryonic kidney 293 (HEK293) cells and Raw264.7 cells were maintained in Dulbecco's modified Eagle medium (DMEM; Gibco BRL, Carlsbad, CA, USA) supplemented with 10% fetal bovine serum (FBS; Gibco BRL) and penicillin/streptomycin (Gibco BRL). Primary osteoblasts were isolated from 4-day-old imprinting control region (ICR) mouse calvaria as described previously,[18] cultured in minimal essential media (α-MEM; Gibco BRL). Active chemical library (LOPAC1280), Alizarin Red S, ascorbic acid, and β-polyglycerolphosphate disodium were purchased from Sigma-Aldrich (St. Louis, MO, USA). The TRACP & ALP Double-Stain Kit was purchased from Takara Bio, Inc. (Shiga, Japan).

Immunoprecipitation and immunoblotting

Immunoprecipitation and immunoblotting were performed as previously described.[19] Cells were harvested, washed in phosphate-buffered saline (PBS; Gibco BRL), and lysed in radioimmunoprecipitation assay (RIPA) buffer (Millipore, Bedford, MA, USA). Proteins were separated by electrophoresis through 10% or 12% SDS PAGE gels, and immunoblotted with specific antibodies. For immunoprecipitation, A/G agarose beads (Thermo Scientific, Waltham, MA, USA) were used.

Murine primary osteoblast differentiation and Alizarin Red staining

Murine primary osteoblasts were seeded, grown to 100% confluence, and then induced to differentiate in α-MEM supplemented with 10 μM β-polyglycerolphosphate disodium and 50 ng/mL ascorbic acid. Cells were treated with I3O at a concentration of 5 or 10 μM. Medium was changed every 2 days for 15 days to achieve differentiation. Cells were washed in PBS, fixed in 4% paraformaldehyde (PFA) for 20 minutes at room temperature, and then stained with 40 μM Alizarin Red.[20] For quantification, Alizarin Red was extracted from stained cells by incubation in 10% acetic acid with shaking for 30 minutes, followed by heating at 85°C for 10 minutes. Acetic acid was neutralized by addition of 10% (v/v) ammonium hydroxide, and samples were centrifuged at $13.5 \times 10^4 g$ for 5 minutes. Absorbance at 405 nm was measured using a spectrophotometer.

Immunocytochemistry

Mouse primary osteoblasts (2.5×10^4/well) were seeded on glass coverslips in a 12-well plate, and I3O was added to the culture 24 hours later after cell stabilization. Cells were washed with PBS and fixed with 4% PFA for 20 minutes at room temperature. After permeabilization with 0.2% Triton X-100 for 15 minutes and blocking with 5% bovine serum albumin (BSA) for 30 minutes, cells were stained for immunofluorescence.

Alkaline phosphatase (ALP) staining

Murine primary osteoblasts were seeded in a 12-well plate at a density of 7×10^4 cells/well and then allowed to differentiate in medium containing I3O for 3 days. Cells were washed with PBS and fixed in 4% PFA for 20 minutes at room temperature and then stained with ALP staining solution (Takara Bio, Inc.) according to the manufacturer's instructions.

Calvaria ex vivo culture and immunohistochemistry

Calvaria were isolated from 4-day-old ICR mice as reported previously.[21] Calvaria were washed with PBS and grown in differentiation medium for 7 days in a 12-well plate on grid. Medium was changed every 2 days. Calvaria were harvested, washed with PBS, and fixed with 4% PFA at 4°C overnight. Decalcification was performed in 4% formic acid and 4% hydrochloric acid (HCl) for 2 days, and 4-μm sections of bone tissue were taken after dehydration and paraffin embedding. Sections were rehydrated in xylene and a graded ethanol series and stained for immunofluorescence. The immunohistochemical analysis of femur sections was performed as described for calvaria staining, with the exception that femur was decalcified in 10% ethylenediaminetetraacetic acid (EDTA), pH 7.4, for 3 weeks, with change of the decalcification solution every 3 days. The number of mononucleated osteoblasts per section was counted from the trabecular bone surface of hematoxylin and eosin (H&E)–stained femur sections.

Differentiation of RAW264.7 cells into osteoclasts in vitro and TRAP staining

Murine macrophage RAW264.7 cells were plated at a density of 1×10^4 cells/well in a 24-well plate and allowed to attach overnight. Cells were treated with 50 ng/mL RANKL in the presence or absence of 10 μM I3O for 4 days, with replacement of medium every 2 days. Cells were then stained using a TRAP assay kit (Sigma-Aldrich) according to the manufacturer's instructions. Co-culture of murine primary osteoblasts and RAW264.7 cells was performed as described previously.[22] TRAP staining of 4-μm sections of femur was performed according to the manufacturer's instructions. Gelatin zymography assay was performed using cell culture supernatants collected from osteoclast-differentiated RAW264.7 cells.

RNA extraction and real-time PCR analysis

Total RNA was isolated from 3-day–differentiated murine primary osteoblasts, and 2 μg of total RNA was reverse transcribed using 200 U reverse transcriptase (Invitrogen, Carlsbad, CA, USA) according to the manufacturer's instructions. The primers used are shown in Supplemental Table S1.

Ovariectomized mouse model

Eight-week-old ICR female mice were obtained from Koatech Laboratories (Seoul, South Korea) and maintained in accordance with the Guide for the Care and Use of Laboratory Animals. All procedures involving mice were approved by the Institutional Animal Care and Use Committee of the Yonsei Laboratory Animal Research Center. Ovariectomy was performed as previously described.[23] Briefly, mice were anesthetized by intraperitoneal (ip) injection of avertin (2-2-2 tribromoethanol; Sigma-Aldrich) and an incision was made on the animal's back. Uterine tubes were tied off with biodegradable thread (to avoid excessive bleeding), followed by removal of ovaries. For sham surgery, the same procedure was performed without removal of ovaries. Each group ($n = 6$) was divided into two subgroups (control and treated). Mice in treated groups were subjected to ip

administration of 10 mg/kg I3O for 6 days/week for a total duration of 4 weeks starting 4 weeks after ovariectomy.

Hindlimb-unloaded mouse model

The hindlimb-unloading (HU) procedure was performed as previously reported.[24] Briefly, 10-week-old male mice ($n = 6$) were placed in individual cages and suspended by the tail using a strip of adhesive surgical tape attached to a chain hanging from the top of the cage. The mice were subjected to hindlimb-unloading for 28 days. I3O treatment (10 mg/kg/day) was initiated 4 days before hindlimb-unloading and administered 6 days/week. Mice were allowed free access to food and water throughout the experiment. After euthanization, the right femurs of the mice were collected for micro-CT analysis.

Micro-CT analysis and cortical bone measurement

After 4 weeks of I3O treatment, femurs were isolated, fixed in 4% PFA, and subjected to micro-CT analysis using a Skyscan model 1076 scanner (Kontich, Belgium) and the following acquisition settings: X-ray source voltage, 70 kVp; current, 140 μA; pixel size, 18 μm; and exposure time, 14.7 seconds. A 0.5-mm-thick aluminum filter was used for beam-hardening reduction, and the rotation step was 0.5° with a complete rotation over 360°. Cortical bone parameters (outer diameter of x axis, outer diameter of y axis, inner diameter, and thickness) were measured using NIS elements AR 3.1 software (Nikon, Tokyo, Japan) of Micro-CT 3D images. Areas of cortical bone were calculated using the mathematical formula for the area of an ellipse ($a \times b \times \pi$, where a = x-axis diameter and b = y-axis diameter). The circumference of the cortical surface was calculated using Ramanujan's formula for ellipse structure.

Statistical analyses

Results were analyzed using Student's t test for comparison of two groups. Statistical significance is defined as $p < 0.05$.

See the Supplemental Materials and Methods for proliferation assay and FACS analysis.

Results

I3O activates Wnt/β-catenin signaling and induces osteogenic differentiation

We screened a chemical library of 1280 pharmacologically active compounds using stable HEK293 cells harboring the Wnt/β-catenin TOPflash reporter.[25] We identified I3O as an activator of the Wnt/β-catenin pathway and checked functionalities of I3O in the differentiation of preosteoblasts and induction of anti-osteoporotic effects. I3O dose-dependently increased β-catenin level in both HEK293 and MC3T3-E1 preosteoblasts (Supplemental Fig. S1*A*), as well as in murine primary osteoblasts (Fig. 1*A*). I3O inhibited the kinase activity of GSK3β, as monitored by levels of p-GSK3β (Ser-9) and p-GSK3β (Y-216), which represent inactive and active statuses of GSK3β, respectively (Supplemental Fig. S1*A*, *B*). I3O disrupted the interactions of both wild-type

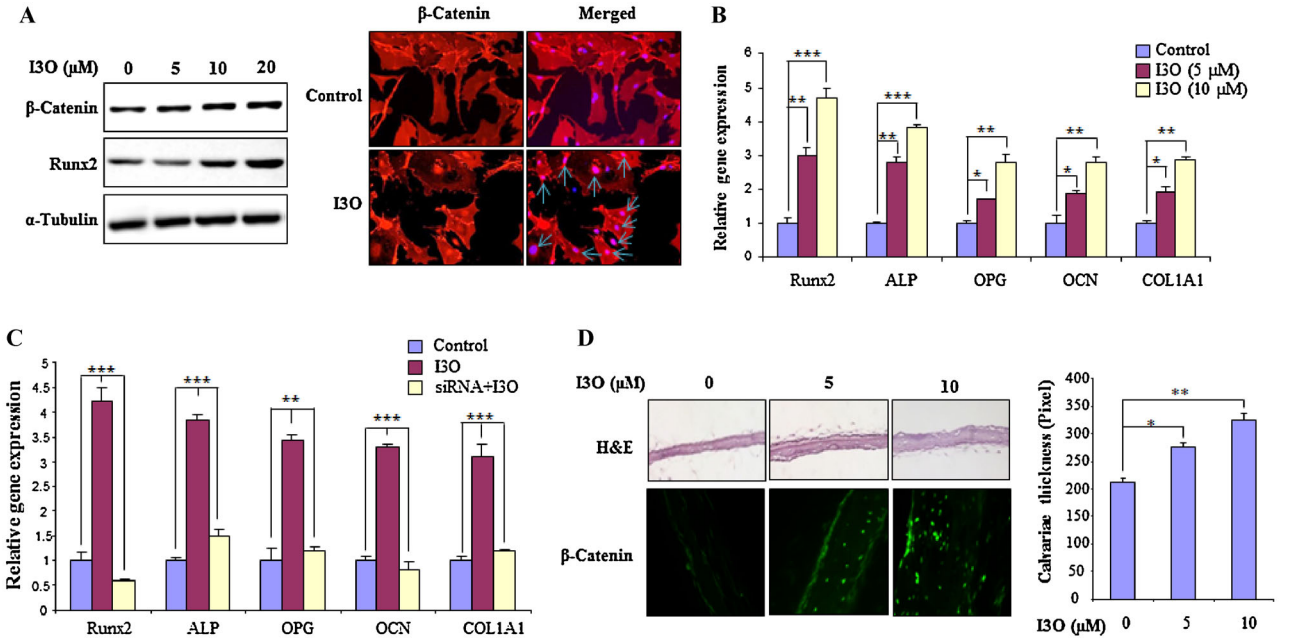

Fig. 1. I3O enhances osteoblast differentiation via the Wnt/β-catenin pathway and stimulates ex vivo calvarial bone growth. (*A*) Murine primary osteoblasts were treated with I3O for 24 hours, followed by immunoblotting analysis to detect β-catenin, RUNX2, and α-tubulin (left panel) and immunofluorescence staining to visualize β-catenin (right panel). (*B*) Murine primary osteoblasts treated with 5 or 10 μM I3O in differentiation medium for 72 hours were subjected to real-time RT-PCR. The expression of genes was normalized to that of GAPDH ($n = 3$). (*C*) Murine primary osteoblasts were treated with control or β-catenin-specific siRNA for 6 hours and then with I3O for an additional 72 hours. Transcription levels of osteogenic genes were measured by real-time RT-PCR, and expression of each gene was normalized to that of GAPDH ($n = 3$). (*D*) Calvarias isolated from 4-day-old ICR mice were treated with I3O in osteogenic differentiation medium for 7 days. Calvarial thickness was assessed by hematoxylin and eosin (H&E) staining (upper panel) and quantified (right panel; $n = 3$). β-catenin was detected by immunofluorescence staining (lower panels) (*B–D*). $^{*}p < 0.05$, $^{**}p < 0.01$, $^{***}p < 0.001$.

and constitutively active mutant GSK3β with β-catenin (Supplemental Fig. S1*B*). Levels of β-catenin and Runt-related transcription factor 2 (RUNX2), a Wnt/β-catenin target gene involved in osteoblast differentiation, were dose-dependently increased in I3O-treated murine primary osteoblasts (Fig. 1*A*, left). I3O also increased the nuclear translocation of β-catenin in these cells (Fig. 1*A*, right). Transcriptional levels of osteogenic differentiation genes, such as *RUNX2*, *ALP*, *OPG*, *OCN*, and *COL1A1*, were also significantly increased by I3O treatment in a dose-dependent manner in murine primary osteoblasts (Fig. 1*B*), whereas β-catenin knockdown by siRNA suppressed transcription of the osteogenic differentiation genes induced by I3O treatment (Supplemental Fig. S2*C*, Fig. 1*C*). I3O also dose-dependently increased ALP activity (Supplemental Fig. S2*A*) and enhanced the mineralization of osteoblasts, as shown by Alizarin Red S staining (Supplemental Fig. S2*B*), whereas it did not affect the proliferation or apoptosis of murine primary osteoblasts, as shown by proliferation (Supplemental Fig. S3*A*) and fluorescence-activated cell sorting (FACS) analyses (Supplemental Fig. S3*B, C*). I3O treatment dose-dependently increased calvarial bone thickness in an ex vivo culture system with increment of nuclear β-catenin (Fig. 1*D*). Collectively, I3O induces osteoblast differentiation in vitro and increases calvarial bone thickness ex vivo with activation of the Wnt/β-catenin pathway.

I3O inhibits osteoclast differentiation in vitro

Wnt/β-catenin signaling plays an important role in the inhibition of osteoclastogenesis.[13] Therefore, we performed a RANKL-induced osteoclast differentiation assay in the murine RAW264.7 macrophage cell line. TRAP staining analysis revealed that I3O suppressed RANKL-induced osteoclastogenesis in RAW264.7 cells, and F-actin staining showed the inhibition of enlarged multinucleated osteoclast formation by I3O treatment (Fig. 2*A*). We also compared the inhibitory effect of I3O on osteoclast differentiation in the RAW264.7 and murine primary osteoblast co-culture system, and accordingly, found I3O-induced inhibition of osteoclast differentiation from RAW264.7 cells (Supplemental Fig. S4).

Moreover, we observed that I3O restored RANKL-induced invasion of murine primary osteoblasts in co-culture with differentiated osteoclasts (Fig. 2*B*) and suppressed RANKL-induced IκBα phosphorylation (Fig. 2*C*).[26]

To confirm the negative effect of I3O on active osteoclastogenesis, we also performed a gelatin zymography assay and found that I3O suppressed the secretion of active matrix metalloproteinase-9 (MMP-9) in RANKL-induced differentiated osteoclasts (Fig. 2*D*). Our results indicate that I3O has a suppressive effect on osteoclast differentiation from RAW264.7 cells in vitro.

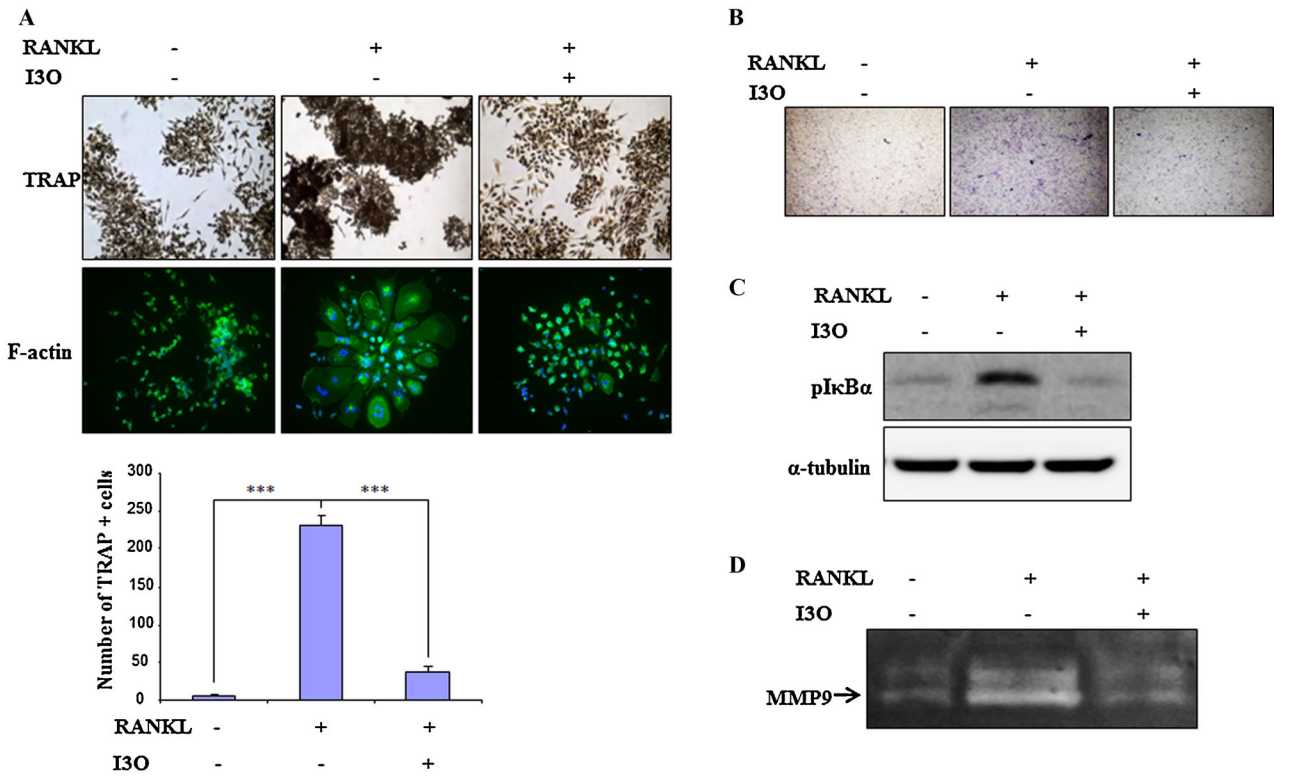

Fig. 2. I3O suppresses RANKL-induced differentiation of RAW264.7 cells into osteoclasts. (*A*) RAW264.7 cells treated with 50 ng/mL RANKL, alone or together with 10 μM I3O, were subjected to ***TRAP*** staining (upper panel) and immunofluorescence staining for F-actin (bottom panel). Nuclei were counterstained with DAPI. TRAP-positive cells were counted ($n = 3$, $^{*}p < 0.05$, $^{**}p < 0.01$, $^{***}p < 0.001$) (lower panels). (*B*) Murine primary osteoblasts grown on Matrigel-coated Transwells were incubated with RANKL, alone or in the presence of co-cultured I3O-treated RAW264.7 cells, and stained with crystal violet after 24 hours. (*C*) RAW264.7 cells were treated with RANKL, alone or together with I3O, for 24 hours and subjected to immunoblotting analysis to detect pIκBα and α-tubulin. (*D*) RAW264.7 cells were treated with RANKL, alone or together with I3O, for 4 days. Conditioned medium was collected and subjected to gelatin zymography assay.

I3O reverses trabecular bone loss in ovariectomized mice

To evaluate whether I3O could overcome excessive bone loss in vivo, we performed sham surgery (Sham) and ovariectomy (Ovx) in 8-week-old mice and allowed 4 weeks for bone loss induction to mimic conditions of postmenopausal osteoporosis (Fig. 3*A*). Mice were then injected ip with I3O and euthanized after 2 weeks or 4 weeks of I3O treatment (Fig. 3*A*). I3O increased bone mass and correlated positively with trabecular bone parameters including bone volume fraction (%) and trabecular thickness (mm) and negatively with trabecular separation in both Sham and Ovx mice (Fig. 3*B–H*). Compared with Ovx mice euthanized after 2 weeks, those euthanized after 4 weeks showed more severe bone loss, as assessed by decreases in bone mineral density, number of trabeculae, and trabecular thickness and separation (Fig. 3*B–H*). The bone mass and density appeared to be markedly further improved in 4-week-treated Sham and Ovx mice (Fig. 3*B–H*). Bone architecture and trabecular bone parameters were completely restored in I3O-treated Ovx mice compared with vehicle-treated Ovx mice (Fig. 3*B–H*). Histomorphometric analysis of mid-diaphyseal bone reflects a constructive effect of I3O on bone mass and trabecular architecture. Additionally, no adverse effects of I3O were observed on body weight or liver histology (Supplemental Fig. S5*A*, *B*). We also examined whether I3O has estrogenic effects on bone, as estrogen is known to have tumor-promoting characteristics.[27] Histological analysis of the uterus showed no significant estrogenic effects of I3O (Supplemental Fig. S5*C*).

I3O increases trabecular bone density and decreases bone resorption

To confirm the effect of I3O on trabecular bone content and bone resorption, we performed histological analysis of femur tissue. Immunofluorescence analysis revealed that β-catenin accumulation was increased in trabecular bone of I3O-treated Sham and Ovx mice compared with vehicle-treated mice (Fig. 4*A*, upper panel). With activation of the Wnt/β-catenin signaling pathway, I3O increased trabecular bone mass and decreased osteoclastogenesis, as demonstrated by H&E and TRAP staining, respectively (Fig. 4*A*, middle and bottom panels). Histomorphometric analysis shows that I3O treatment increased the number of osteoblasts on trabecular bone surface in sham as well as in the ovx mouse group along with an increased number of osteocytes, indicating that I3O does not only increase the number of osteoblasts but also enhances osteoblast activity (Supplemental Fig. S6*A–C*). The expression of osteogenic genes such as *ALP, RUNX2, COL1*, and *OCN* were increased in I3O-treated Sham and Ovx mice compared with vehicle-treated Sham and Ovx mice (Fig. 4*B–E*). The ratio of RANKL, a secreted osteoclastogenesis activator, to

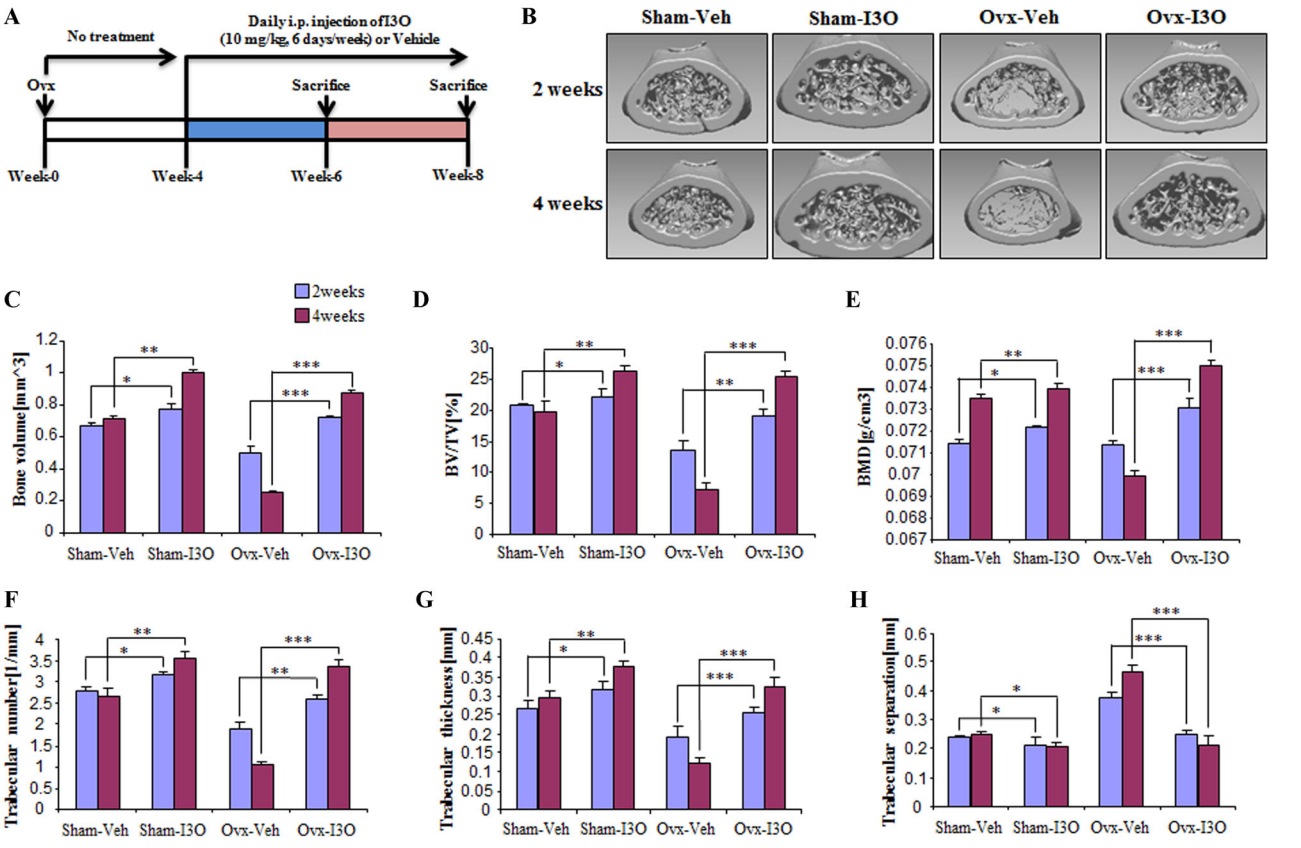

Fig. 3. I3O reverses bone loss and increases bone formation in the ovariectomized (Ovx) mouse model. (*A*) Schematic diagram of in vivo experiments. I3O (10 mg/kg/d) was administered 4 weeks after ovariectomy in ICR female mice, and the mice were euthanized 2 or 4 weeks after ip injection ($n = 6$). (*B–H*) Micro-CT scanning of right femurs was performed, and 3D images of trabecular and cortical bone were constructed. Bone quality was evaluated by measurement of trabecular bone parameters bone volume (*C*), bone volume to tissue volume ratio (BV/TV) (*D*), bone mineral density (BMD) (*E*), number of trabeculae (*F*), trabecular thickness (*G*), and trabecular separation (*H*). (*C–H*) $^{*}p < 0.05$, $^{**}p < 0.01$, $^{***}p < 0.001$.

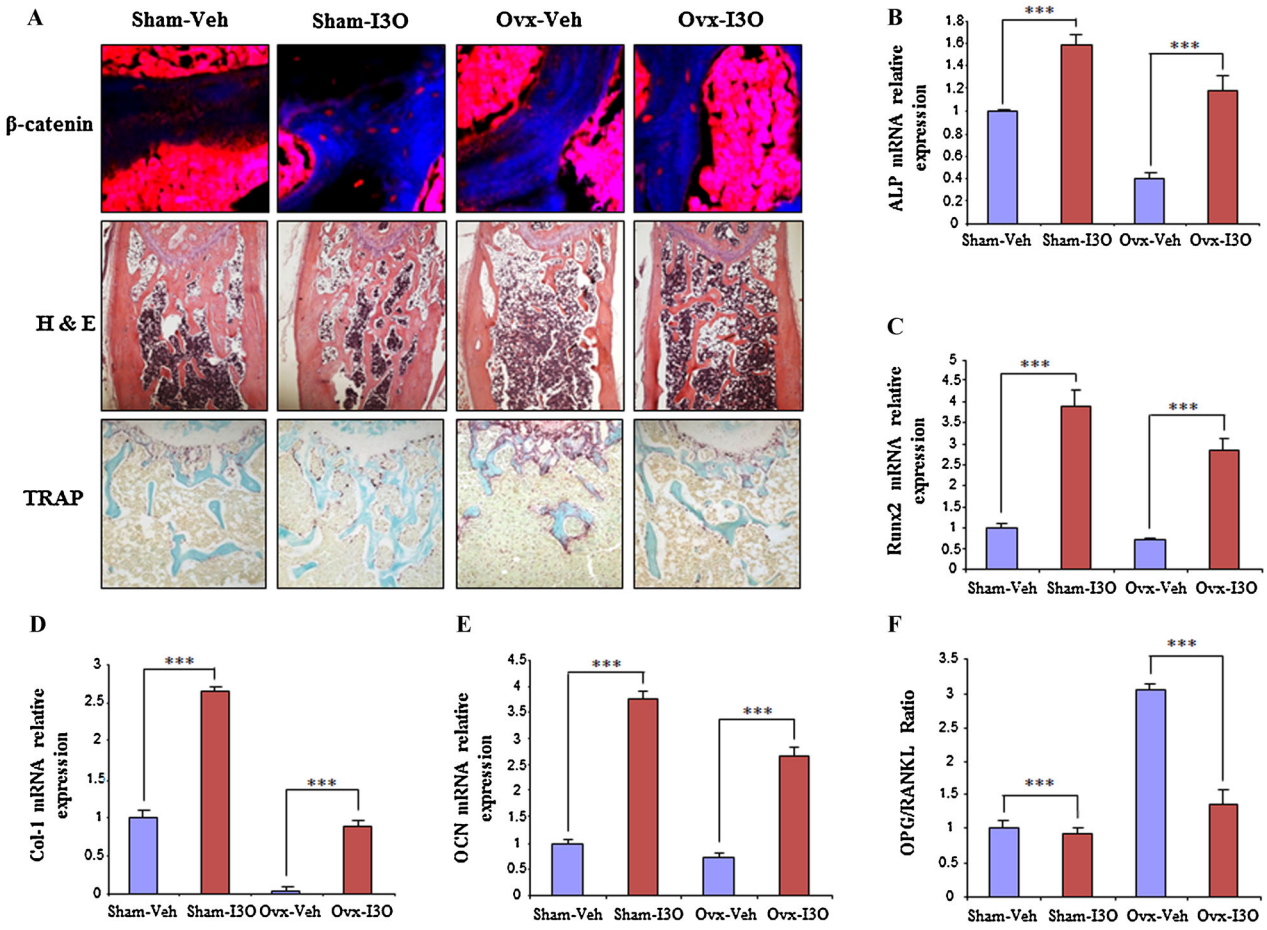

Fig. 4. I3O enhances trabecular bone density and osteogenic gene expression in OVX mouse femur. (*A*) Sections of femurs from mice treated with vehicle or I3O for 4 weeks were subjected to immunofluorescence staining to detect β-catenin (upper panel), or H&E staining (middle panel) and TRAP staining (bottom panel) to assess bone resorption. Femurs isolated from mice treated for 4 weeks were analyzed by real-time RT-PCR to detect the expression levels of ALP (*B*), RUNX2 (*C*), COL1A1 (*D*), OCN (*E*), or OPG to RANKL ratio (*F*). (*B–F*) $^{*}p < 0.05$, $^{**}p < 0.01$, $^{***}p < 0.001$.

OPG, a secreted osteoclastogenesis inhibitor, was decreased dose-dependently by I3O treatment in femur tissue of Ovx mice (Fig. 4*F*). Collectively, our data show that I3O increases trabecular bone content and decreases bone resorption, with increased accumulation of β-catenin, in I3O-treated Sham and Ovx mice.

I3O enhances cortical bone thickness

Cortical bone thickness and area reflect bone strength.[28] We evaluated the effect of I3O on cortical bone using these measurements. The cortical bone thickness, cortical bone total surface area, cortical bone inner surface area, and inner and outer circumference were measured as shown by the representative micro-CT images (Fig. 5*A*). Measurements of the corresponding parameters showed reduction in thickness and total and inner area of cortical bone in Ovx mice compared with those of Sham mice; however, I3O restored those cortical bone parameters reduced by Ovx to the levels of Sham mice (Fig. 5*B–D*). In addition, I3O treatment showed an increased effect on cortical bone in I3O-treated Sham mice compared with vehicle-treated Sham mice in 4 weeks (Fig. 5*B–D*). I3O treatment also shows a promoting effect on cortical outer and inner circumferences in the Sham as well as in the Ovx mouse group, whereas vehicle-treated Ovx mice show reduction in outer and inner cortical bone circumferences (Fig. 5*E*, *F*). Immunofluorescence analyses showed an increased accumulation of β-catenin in cortical bone of both I3O-treated Sham and Ovx mice (Fig. 5*G*). Overall, a net increment in the circumference, area, and thickness of cortical bone indicates that quality of bones pertaining to their strength is improved by I3O.

I3O restores normal bone density in a hindlimb-unloaded mouse model

Bone loss in non-age–related osteoporosis is induced by long-term immobilization or long-term exposure to microgravity.[29] To mimic the non-age–related osteoporotic condition, we used an HU mouse model and tested an effect of I3O on bone density. Mice were suspended for a period of 28 days starting on the fifth day of I3O treatment (Fig. 6*A*). HU induced trabecular bone loss in suspended mice, as shown by micro-CT analysis, and trabecular bone parameters were restored by I3O treatment (Fig. 6*B–H*). Bone volume, bone volume fraction (%), bone mineral density (g/cm^3), trabecular thickness (mm), and number of trabeculae

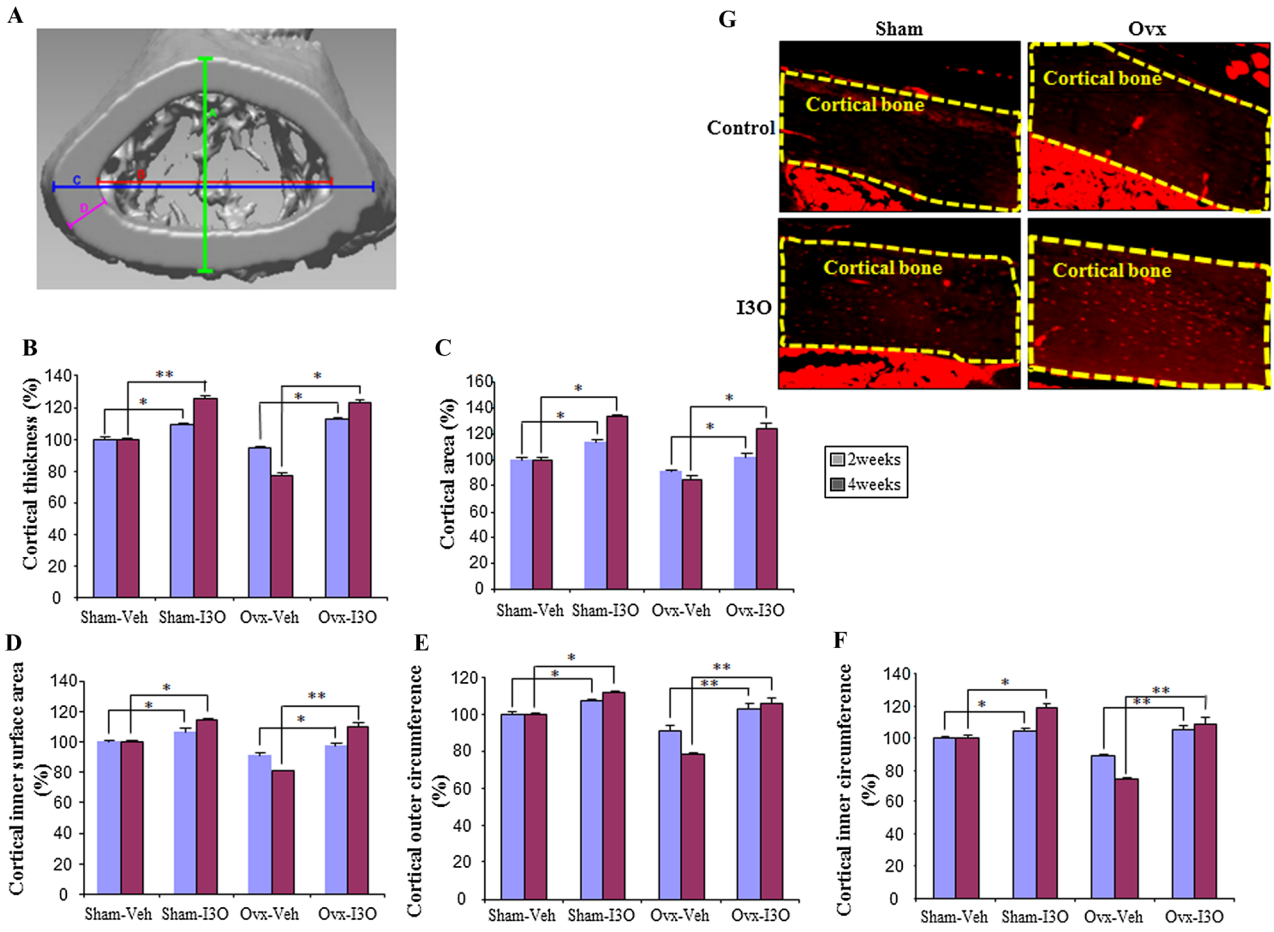

Fig. 5. I3O increases cortical bone through activation of Wnt/β-catenin signaling. (*A*) Schematic diagram of cortical bone measurement: a, y axis of outer diameter (light green); b, x axis of inner diameter (red); c, x axis of outer diameter (blue); d, cortical thickness (violet). Relative parameters of cortical thickness (*B*), cortical total surface area (*C*), cortical inner surface area (*D*), cortical outer circumference (*E*), and cortical inner circumference (*F*) of femur from mice treated for 2 and 4 weeks ($n = 6$). (*B–E*) $^{*}p < 0.05$, $^{**}p < 0.01$, $^{***}p < 0.001$. (*G*) Immunofluorescence staining of β-catenin in cortical bone. Areas marked by yellow dotted lines are the regions of cortical bones treated with vehicle or I3O for 4 weeks.

were significantly decreased in HU mice and were restored by I3O treatment. Increased trabecular separation (mm) induced by hindlimb unloading was also restored to baseline by I3O in the suspended mice (Fig. 6*B–H*). Overall, I3O has restorative effects on bone loss induced by either hindlimb unloading or ovariectomy in mice.

Discussion

The inhibition of GSK3β is one of the major means of activating Wnt/β-catenin signaling.[14] Therefore, GSK3β has been considered a potential therapeutic target for metabolic bone diseases, such as osteoporosis. As a known ATP-competitive kinase inhibitor of GSK3β, I3O directly interacts with the ATP-binding pocket of GSK3β.[30] By binding GSK3β, I3O abolishes the capacity of GSK3β to bind to β-catenin and inhibits the kinase activity of GSK3β. I3O is an analog of indirubin, a Chinese medicine used for the treatment of leukemia, and shows potent inhibitory activity against cyclin-dependent kinases.[30] I3O also has antitumor activity and induces growth arrest and apoptosis in cancer cells.[31,32] However, we did not observe any discernible effects of I3O on proliferation and apoptosis in osteoblasts after treatment in vitro with 10 μM, the concentration used for the induction of osteoblast differentiation.

Application of I3O up to a concentration of 20 mg/kg in an in vivo mouse model has also been shown to be nontoxic,[33] suggesting that I3O is safe. In our study, we also tested I3O for any potential toxicity in highly fragile neural stem cells (data not shown), and consistent with our in vivo findings, I3O treatment at the concentration of 10 μM did not show any adverse effects.

Wnt/β-catenin signaling has an established role in regulation of bone mass by maintaining a balance between bone formation and resorption. Wnt/β-catenin signaling negatively regulates osteoclast formation by inducing secretion of OPG by osteoblasts and leading to sequestration of RANKL by OPG and subsequent neutralization of RANKL.[13] These reports indicate that osteoblasts are key mediators of the inhibition of osteoclastogenesis by Wnt/β-catenin signaling.[34] However, a recent report shows that Wnt/β-catenin signaling can also inhibit osteoclastogenesis independent of osteoblasts.[35] We found osteoblast-independent inhibition of osteoclastogenesis by Wnt/β-catenin signaling; I3O suppresses differentiation of

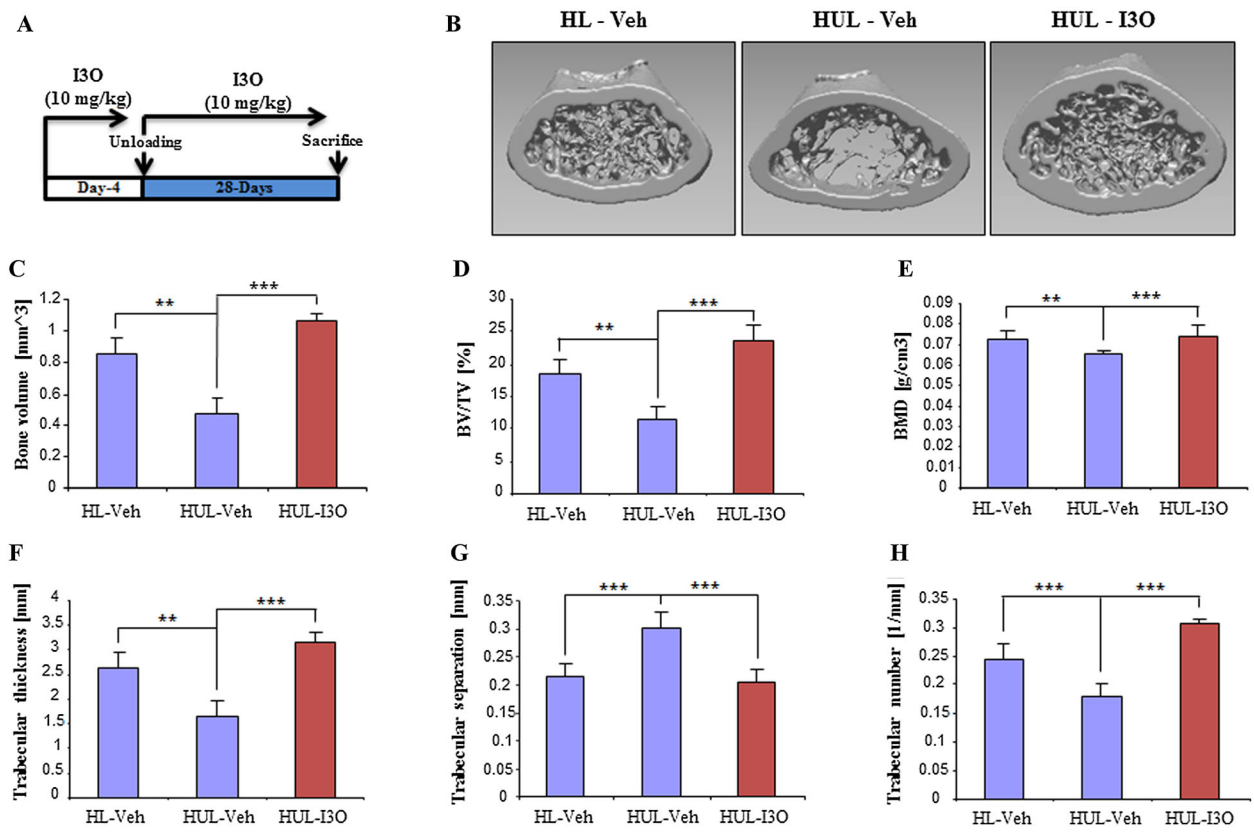

Fig. 6. I3O restores bone density in a hindlimb-unloaded mouse model. (*A*) Schematic diagram of hindlimb-unloading experiments with I3O treatment. (*B*) Right femurs of 4-week hindlimb-unloaded and control mice were subjected to micro-CT scanning analysis, and 3D images were constructed using the CT data ($n = 6$). (*C*) Micro-CT morphometric analysis of trabecular bones of 4-week hindlimb-unloaded and control mouse femurs. Bone quality was evaluated by the measurement of the trabecular bone parameters bone volume (*C*), bone volume to tissue volume ratio (BV/TV) (*D*), bone mineral density (BMD) (*E*), trabecular thickness (*F*), trabecular separation (*G*), and number of trabeculae (*H*). (*C–H*) $^{*}p < 0.05$, $^{**}p < 0.01$, $^{***}p < 0.001$.

RAW264.7 cells into osteoclasts, even in the absence of osteoblasts in vitro, and also impedes trabecular bone resorption in ovariectomized mice in vivo.

Increased invasion and migration of osteoblasts induced by osteoclasts have been illustrated,[22,36] and MMP-9 is known to induce invasion and migration of osteoblasts.[37,38] In this study, we provide evidence of I3O's inhibitory effect on osteoclastogenesis in vitro; I3O was shown to inhibit RANKL-induced MMP-9 secretion and arrest osteoblast cell invasion.

In the Ovx mouse model, I3O significantly restored bone loss, improved bone quality back to baseline levels within 2 weeks, and further increased bone mass for 4 weeks. These results indicate that I3O can restore bone mass back to baseline levels in osteoporotic individuals even with treatment of short duration. Therefore, I3O could be an attractive short-term therapeutic agent for osteoporotic patients for its effective response, although applicability as a discontinuous therapy for osteoporosis needs to be tested.

The thickness and area of cortical bone are other key parameters in determining bone strength[28] and are usually reduced after ovariectomy.[39] We found that I3O increased area and thickness of cortical bone, resulting in increased bone strength. Interestingly, both mass and quality of bone were improved in the normal mice treated with I3O, indicating that I3O retains function for the prevention of osteoporosis. In addition, we did not observe any side effects, such as hyperclyemia, toxicity, or severe body-weight loss with I3O application in normal mice.

Hindlimb-unloading is a model for skeletal muscle atrophy and bone loss.[40] Hindlimb-unloading causes bone resorption and decreased bone formation, and results in reduction in bone density.[24] Treatment with I3O was shown to reverse the bone loss and restore bone mass density in HU mice compared with control suspended mice.

Treatment with bone resorption inhibitors, such as bisphosphonates, induce osteonecrosis[41] and higher risks of esophagitis and myalgia, and estrogen replacement therapy carries increased risks of deep vein thrombosis, cardiovascular disease, and breast cancer.[42] It was recently reported that combinatorial therapy using the resorption inhibitor denosumab and anabolic agent PTH increased bone density to a greater extent than either agent alone.[43]

In such a context, the pharmacologically active small molecule I3O would be more effective, as it shows a significant inhibitory effect on bone resorption and an anabolic effect on bone formation. Thus, I3O, showing the additional advantage of antitumor activity, could be developed as a promising anti-osteoporosis anabolic agent without potential risks of cancer development.

Disclosures

All authors state that they have no conflicts of interest.

Acknowledgments

This project was partially or fully sponsored by grants from the National Research Foundation (NRF), funded by the Ministry of Future Creation and Science (MFCS) of Korea, Mid-career Researcher Program (2012-010285), and Translational Research Center for Protein Function Control (2009-0083522). This work was also supported by a grant of the Korea Research Institute of Chemical Technology (SI-095).

Authors' roles: All authors contributed equally to the development of this article, providing intellectual input into the content and design, critically reviewing it, and giving final approval.

References

1. Cheung AM, Feig DS, Kapral M, Diaz-Granados N, Dodin S. Canadian Task Force on Preventive Health C. Prevention of osteoporosis and osteoporotic fractures in postmenopausal women: recommendation statement from the Canadian Task Force on Preventive Health Care. Can Med Assoc J. 2004;170(11):1665–7.
2. Sontag A, Krege JH. First fractures among postmenopausal women with osteoporosis. J Bone Miner Metab. 2010;28(4):485–8.
3. Cummings SR, Melton LJ. Epidemiology and outcomes of osteoporotic fractures. Lancet. 2002;359(9319):1761–7.
4. Mnif H, Koubaa M, Zrig M, Trabelsi R, Abid A. Elderly patients' mortality and morbidity following trochanteric fracture. A prospective study of 100 cases. Orthop Traumatol Surg Res. 2009;95(7):505–10.
5. Khandewal S, Chandra M, Lo JC. Clinical characteristics, bone mineral density and non-vertebral osteoporotic fracture outcomes among post-menopausal U.S. South Asian women. Bone. 2012;51(6):1025–8.
6. Sugimoto M, Futaki N, Harada M, Kaku S. Effects of combined treatment with eldecalcitol and alendronate on bone mass, mechanical properties, and bone histomorphometry in ovariectomized rats: a comparison with alfacalcidol and alendronate. Bone. 2013;52(1):181–8.
7. LeBlanc A, Schneider V, Shackelford L, et al. Bone mineral and lean tissue loss after long duration space flight. J Musculoskelet Neuronal Interact. 2000;1(2):157–60.
8. Armbrecht G, Belavy DL, Backstrom M, et al. Trabecular and cortical bone density and architecture in women after 60 days of bed rest using high-resolution pQCT: WISE 2005. J Bone Miner Res. 2011;26(10):2399–410.
9. Piters E, Boudin E, Van Hul W. Wnt signaling: a win for bone. Arch Biochem Biophys. 2008;473(2):112–6.
10. Gong Y, Slee RB, Fukai N, et al. LDL receptor-related protein 5 (LRP5) affects bone accrual and eye development. Cell. 2001;107(4):513–23.
11. Ai M, Holmen SL, Van Hul W, Williams BO, Warman ML. Reduced affinity to and inhibition by DKK1 form a common mechanism by which high bone mass-associated missense mutations in LRP5 affect canonical Wnt signaling. Mol Cell Biol. 2005;25(12):4946–55.
12. Glass DA 2nd, Bialek P, Ahn JD, et al. Canonical Wnt signaling in differentiated osteoblasts controls osteoclast differentiation. Dev Cell. 2005;8(5):751–64.
13. Krishnan V, Bryant HU, Macdougald OA. Regulation of bone mass by Wnt signaling. J Clin Invest. 2006;116(5):1202–9.
14. Clevers H, Nusse R. Wnt/beta-catenin signaling and disease. Cell. 2012;149(6):1192–205.
15. Cai Y, Mohseny AB, Karperien M, Hogendoorn PC, Zhou G, Cleton-Jansen AM. Inactive Wnt/beta-catenin pathway in conventional high-grade osteosarcoma. J Pathol. 2010;220(1):24–33.
16. Hoeppner LH, Secreto FJ, Westendorf JJ. Wnt signaling as a therapeutic target for bone diseases. Expert Opin Ther Targets. 2009;13(4):485–96.
17. Clement-Lacroix P, Ai M, Morvan F, et al. Lrp5-independent activation of Wnt signaling by lithium chloride increases bone formation and bone mass in mice. Proc Natl Acad Sci USA. 2005;102(48):17406–11.
18. Wang YH, Liu Y, Buhl K, Rowe DW. Comparison of the action of transient and continuous PTH on primary osteoblast cultures expressing differentiation stage-specific GFP. J Bone Miner Res. 2005;20(1):5–14.
19. Jeong WJ, Yoon J, Park JC, et al. Ras stabilization through aberrant activation of Wnt/beta-catenin signaling promotes intestinal tumorigenesis. Sci Signal. 2012;5(219):ra30.
20. Yamaguchi M, Weitzmann MN. The bone anabolic carotenoid p-hydroxycinnamic acid promotes osteoblast mineralization and suppresses osteoclast differentiation by antagonizing NF-kappaB activation. Int J Mol Med. 2012;30(3):708–12.
21. Garrett IR, Mundy GR. The role of statins as potential targets for bone formation. Arthritis Res. 2002;4(4):237–40.
22. Sanchez-Fernandez MA, Gallois A, Riedl T, Jurdic P, Hoflack B. Osteoclasts control osteoblast chemotaxis via PDGF-BB/PDGF receptor beta signaling. PloS One. 2008;3(10):e3537.
23. Alexander JM, Bab I, Fish S, et al. Human parathyroid hormone 1–34 reverses bone loss in ovariectomized mice. J Bone Miner Res. 2001;16(9):1665–73.
24. Wang X, Guo B, Li Q, et al. miR-214 targets ATF4 to inhibit bone formation. Nat Med. 2013;19(1):93–100.
25. Lee SH, Kim B, Oh MJ, et al. Persicaria hydropiper (L.) spach and its flavonoid components, isoquercitrin and isorhamnetin, activate the Wnt/beta-catenin pathway and inhibit adipocyte differentiation of 3T3-L1 cells. Phytother Res. 2011;25(11):1629–35.
26. Ang E, Pavlos NJ, Rea SL, et al. Proteasome inhibitors impair RANKL-induced NF-kappaB activity in osteoclast-like cells via disruption of p62, TRAF6, CYLD, and IkappaBalpha signaling cascades. J Cell Physiol. 2009;220(2):450–9.
27. Finan B, Yang B, Ottaway N, et al. Targeted estrogen delivery reverses the metabolic syndrome. Nat Med. 2012;18(12):1847–56.
28. Davison KS, Siminoski K, Adachi JD, et al. Bone strength: the whole is greater than the sum of its parts. Semin Arthritis Rheum. 2006;36(1):22–31.
29. Visigalli D, Strangio A, Palmieri D, Manduca P. Hind limb unloading of mice modulates gene expression at the protein and mRNA level in mesenchymal bone cells. BMC Musculoskelet Disord. 2010;11:147.
30. Leclerc S, Garnier M, Hoessel R, et al. Indirubins inhibit glycogen synthase kinase-3 beta and CDK5/p25, two protein kinases involved in abnormal tau phosphorylation in Alzheimer's disease. A property common to most cyclin-dependent kinase inhibitors? J Biol Chem. 2001;276(1):251–60.
31. Hoessel R, Leclerc S, Endicott JA, et al. Indirubin, the active constituent of a Chinese antileukaemia medicine, inhibits cyclin-dependent kinases. Nat Cell Biol. 1999;1(1):60–7.
32. Duensing S, Duensing A, Lee DC, et al. Cyclin-dependent kinase inhibitor indirubin-3′-oxime selectively inhibits human papillomavirus type 16 E7-induced numerical centrosome anomalies. Oncogene. 2004;23(50):8206–15.
33. Chiara F, Gambalunga A, Sciacovelli M, et al. Chemotherapeutic induction of mitochondrial oxidative stress activates GSK-3alpha/beta and Bax, leading to permeability transition pore opening and tumor cell death. Cell Death Dis. 2012;3:e444.
34. Spencer GJ, Utting JC, Etheridge SL, Arnett TR, Genever PG. Wnt signalling in osteoblasts regulates expression of the receptor activator of NFkappaB ligand and inhibits osteoclastogenesis in vitro. J Cell Sci. 2006;119(Pt 7):1283–96.
35. Albers J, Keller J, Baranowsky A, et al. Canonical Wnt signaling inhibits osteoclastogenesis independent of osteoprotegerin. J Cell Biol. 2013;200(4):537–49.
36. Hughes A, Kleine-Albers J, Helfrich MH, Ralston SH, Rogers MJ. A class III semaphorin (Sema3e) inhibits mouse osteoblast migration and decreases osteoclast formation in vitro. Calcif Tissue Int. 2012;90(2):151–62.

37. Wang L, Zhang ZG, Zhang RL, et al. Matrix metalloproteinase 2 (MMP2) and MMP9 secreted by erythropoietin-activated endothelial cells promote neural progenitor cell migration. J Neurosci. 2006; 26(22):5996–6003.
38. Dufour A, Zucker S, Sampson NS, Kuscu C, Cao J. Role of matrix metalloproteinase-9 dimers in cell migration: design of inhibitory peptides. J Biol Chem. 2010;285(46):35944–56.
39. Ominsky MS, Stouch B, Schroeder J, et al. Denosumab, a fully human RANKL antibody, reduced bone turnover markers and increased trabecular and cortical bone mass, density, and strength in ovariectomized cynomolgus monkeys. Bone. 2011;49(2):162–73.
40. Bloomfield SA, Allen MR, Hogan HA, Delp MD. Site- and compartment-specific changes in bone with hindlimb unloading in mature adult rats. Bone. 2002;31(1):149–57.
41. Kang B, Cheong S, Chaichanasakul T, et al. Periapical disease and bisphosphonates induce osteonecrosis of the jaws in mice. J Bone Miner Res. 2013;28(7):1631–40.
42. Rosen CJ. Clinical practice. Postmenopausal osteoporosis. N Engl J Med. 2005;353(6):595–603.
43. Tsai JN, Uihlein AV, Lee H, et al. Teriparatide and denosumab, alone or combined, in women with postmenopausal osteoporosis: the DATA study randomised trial. Lancet. 2013;382(9886):50–6.